

## Third Order Calculation of Beam Position

Rob Kutschke, CD/EXP

### Abstract

This note works out the third order estimate for the beam position, for use with the upgraded Tevatron BPMs, including corrections for the un-measured coordinate. The note includes figures that illustrate the residual error that remains after the corrections are made. Code to implement the correction has been placed in the DocDB along with this writeup. The main result of the paper is in Figure 5, which shows the accuracy that can be achieved online and Figure 6, which shows the accuracy that can be achieved offline. There is one important caveat: the treatment of the coupling between the electrodes may not be complete.

## 1 Caveat

This note does not do a complete treatment of the coupling between the electrodes in the pickup. Hopefully a more complete treatment will only change the details, not the big picture.

## 2 Model Without Coupling

In Beams-doc-1161-v1, equation 6 gives the magnitudes of the  $A$  and  $B$  signals on a pickup as a function of beam position and current. The model ignores the coupling between the electrodes and any edge effects coming from the finite length of the electrodes. The model is,

$$A_0 = \frac{I_A}{I_{\text{beam}}} = \frac{\phi}{2\pi} \left( 1 + \sum_{n=1}^{\infty} \frac{4}{n\phi} \left( \frac{r}{b} \right)^n \cos(n\theta) \sin\left(n\frac{\phi}{2}\right) \right) \quad (1)$$

$$B_0 = \frac{I_B}{I_{\text{beam}}} = \frac{\phi}{2\pi} \left( 1 + \sum_{n=1}^{\infty} \frac{4}{n\phi} \left( \frac{r}{b} \right)^n \cos(n\theta) \sin\left(n\left(\pi + \frac{\phi}{2}\right)\right) \right), \quad (2)$$

where the actual beam position is given in 2D polar coordinates  $(r, \theta)$ , where  $b$  is the radius of curvature of the electrodes and where the electrodes subtend an arc of angle  $\phi$ . The origin of the coordinate system has been chosen so that  $x$  is the coordinate measured by the BPM while  $y$  is the orthogonal coordinate. These quantities are illustrated in Figure 1. The subscript 0 on  $A_0$  and  $B_0$  indicates that these quantities ignore coupling.

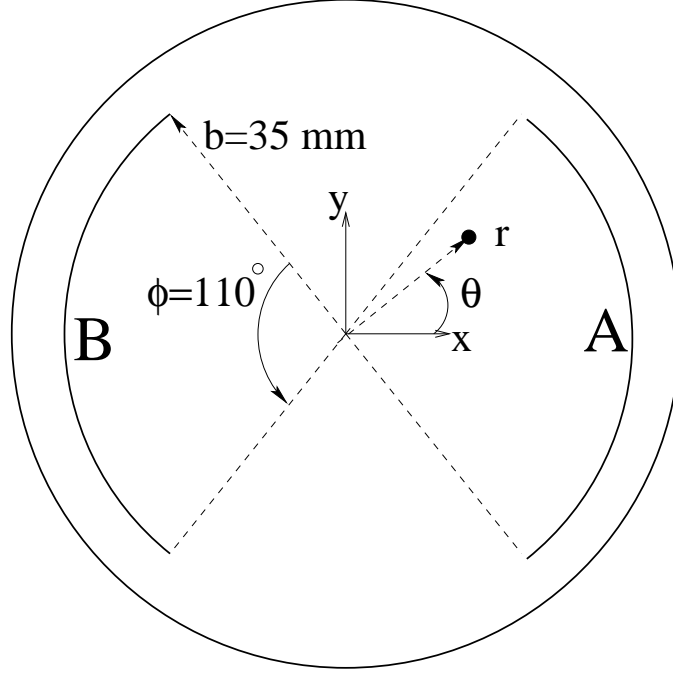


Figure 1: Definition of the parameters used in the equations. The two electrodes are labeled *A* and *B*. The electrodes are concentric arcs of a circle of radius  $b$ . The angle subtended by each electrode is given by  $\phi$ . The BPM measures the  $x$  coordinate. The beam position is indicated by the filled dot and its position is denoted by either  $(x, y)$  or  $(r, \theta)$ . The numerical values come from Beams-doc-809.

Expanding these equations to third order in  $r/b$  gives,

$$A_0 = \frac{\phi}{2\pi} \left( 1 + \frac{4}{\phi} \frac{r}{b} \cos \theta \sin \left( \frac{\phi}{2} \right) + \frac{4}{2\phi} \left( \frac{r}{b} \right)^2 \cos(2\theta) \sin(\phi) + \frac{4}{3\phi} \left( \frac{r}{b} \right)^3 \cos(3\theta) \sin \left( \frac{3\phi}{2} \right) + \dots \right) \quad (3)$$

$$B_0 = \frac{\phi}{2\pi} \left( 1 + \frac{4}{\phi} \frac{r}{b} \cos \theta \sin \left( \pi + \frac{\phi}{2} \right) + \frac{4}{2\phi} \left( \frac{r}{b} \right)^2 \cos(2\theta) \sin \left( 2\left( \pi + \frac{\phi}{2} \right) \right) + \frac{4}{3\phi} \left( \frac{r}{b} \right)^3 \cos(3\theta) \sin \left( 3\left( \pi + \frac{\phi}{2} \right) \right) + \dots \right) \quad (4)$$

$$= \frac{\phi}{2\pi} \left( 1 - \frac{4}{\phi} \frac{r}{b} \cos \theta \sin \left( \frac{\phi}{2} \right) + \frac{4}{2\phi} \left( \frac{r}{b} \right)^2 \cos(2\theta) \sin(\phi) - \frac{4}{3\phi} \left( \frac{r}{b} \right)^3 \cos(3\theta) \sin \left( \frac{3\phi}{2} \right) + \dots \right) \quad (5)$$

In the last line, the only change is to reduce the  $\sin \phi$  terms. These equations can be changed to Cartesian coordinates using,

$$\cos(2\theta) = \cos^2 \theta - \sin^2 \theta \quad (6)$$

$$\cos(3\theta) = \cos(2\theta + \theta) \quad (7)$$

$$= \cos(2\theta) \cos(\theta) - \sin(2\theta) \sin(\theta) \quad (8)$$

$$= (\cos^2 \theta - \sin^2 \theta) \cos \theta - 2 \sin \theta \cos \theta \sin \theta \quad (9)$$

$$= \cos \theta (\cos^2 \theta - 3 \sin^2 \theta). \quad (10)$$

This gives,

$$A_0 = \frac{\phi}{2\pi} (1 + a_1 x + a_2(x^2 - y^2) + a_3 x(x^2 - 3y^2)) \quad (11)$$

$$B_0 = \frac{\phi}{2\pi} (1 - a_1 x + a_2(x^2 - y^2) - a_3 x(x^2 - 3y^2)), \quad (12)$$

where,

$$a_1 = \frac{4}{\phi b} \sin \left( \frac{\phi}{2} \right) \quad (13)$$

$$a_2 = \frac{2}{\phi b^2} \sin(\phi) \quad (14)$$

$$a_3 = \frac{4}{3\phi b^3} \sin \left( \frac{3\phi}{2} \right). \quad (15)$$

### 3 Adding Linear Coupling

If the electrodes  $A$  and  $B$  are linearly coupled, then the signals on  $A$  and  $B$  are given by,

$$A = A_0 + CB \quad (16)$$

$$B = B_0 + CA, \quad (17)$$

where  $A$  and  $B$  are the signals including coupling and where  $C$  is the coupling coefficient.  $A_0$  and  $B_0$ , the signals in the no-coupling limit, are given by equations 11 and 12, respectively. The solution to these equations is,

$$A = \frac{A_0 + CB_0}{1 - C^2} \quad (18)$$

$$B = \frac{B_0 + CA_0}{1 - C^2} \quad (19)$$

Expanding to third order in  $r/b$  gives,

$$A = \frac{\phi}{2\pi} \frac{1}{1 - C} (1 + b_1 x + b_2(x^2 - y^2) + b_3 x(x^2 - 3y^2)) \quad (20)$$

$$B = \frac{\phi}{2\pi} \frac{1}{1 - C} (1 - b_1 x + b_2(x^2 - y^2) - b_3 x(x^2 - 3y^2)), \quad (21)$$

where,

$$b_1 = a_1 \frac{1 - C}{1 + C} = \frac{4}{\phi b} \sin\left(\frac{\phi}{2}\right) \frac{1 - C}{1 + C} \quad (22)$$

$$b_2 = a_2 = \frac{2}{\phi b^2} \sin(\phi) \quad (23)$$

$$b_3 = a_3 \frac{1 - C}{1 + C} = \frac{4}{3\phi b^3} \sin\left(\frac{3\phi}{2}\right) \frac{1 - C}{1 + C}. \quad (24)$$

## 4 First Order Position and the Value of $b$

To first order in  $r/b$ , Equations 20 and 21 give the familiar expression for the position as a function of  $A$  and  $B$ ,

$$x_1 = \frac{1}{b_1} \frac{A - B}{A + B}, \quad (25)$$

where the subscript 1 on  $x_1$  denotes that this is the first order estimate. From bench test measurements we know that  $1/b_1 = 26$  mm to an accuracy of a few %. Using this value, Equation 22 can be solved for  $C$ ,

$$C = \frac{a_1 - b_1}{a_1 + b_1} = 0.11810 \quad (26)$$

We can also write Equation 22 in terms of an effective radius,  $b_{\text{eff}}$ ,

$$b_1 = \frac{4}{\phi b_{\text{eff}}} \sin\left(\frac{\phi}{2}\right). \quad (27)$$

Solving this for  $b_{\text{eff}}$  gives,

$$b_{\text{eff}} = b \frac{1 + C}{1 - C} = 44.37 \text{ mm}. \quad (28)$$

As expected  $b_{\text{eff}}$  is larger than the physical radius of 35 mm. Using this value of  $C$  provides enough information to determine the values of the  $b$  coefficients,

$$b_1 = 3.8461 \times 10^{-2} \text{ mm}^{-1} \quad (29)$$

$$b_2 = 6.3030 \times 10^{-4} \text{ mm}^{-2} \quad (30)$$

$$b_3 = 3.3067 \times 10^{-6} \text{ mm}^{-3} \quad (31)$$

$$r_{31} = b_3/b_1 = 8.5975 \times 10^{-5} \text{ mm}^{-2}. \quad (32)$$

## 5 Third Order Position

Using Equations 20 and 21 one can obtain an expression for the third order estimate for the position,  $x_3$ ,

$$\frac{1}{b_1} \frac{A - B}{A + B} = x_3 \frac{1 + r_{31}(x_3^2 - 3y^2)}{1 + b_2(x_3^2 - y^2)}, \quad (33)$$

where  $r_{31} = b_3/b_1$ . The left hand side can be identified as the first order position estimate,  $x_1$ . If independent knowledge of  $y$  is available, this equation can be solved for  $x_3$ ,

$$x_1(1 + a_2(x_3^2 - y^2)) = x_3(1 + r_{31}(x_3^2 - 3y^2)) \quad (34)$$

$$x_1 + x_1 a_2 x_3^2 - x_1 a_2 y^2 = x_3 + r_{31} x_3^3 - 3r_{31} x_3 y^2 \quad (35)$$

$$x_3^3 - \frac{x_1 a_2}{r_{31}} x_3^2 + \frac{(1 - 3r_{31} y^2)}{r_{31}} x_3 - \frac{x_1(1 - a_2 y^2)}{r_{31}} = 0. \quad (36)$$

This cubic equation can be solved using a library routine such as the CERNLIB routine DRTEQ3. Inside the domain  $|x_3| < 22$  mm and  $|y| < 22$  mm, the cubic equation always has one real root and two complex roots; the real root is the unique choice for the solution. As either  $x$  or  $y$  approach  $b$ , the cubic equation has three real roots and it is not immediately obvious which is the correct one. However that situation has never occurred during extensive simulation of this model.

In order to solve the cubic equation, one requires an independent estimate of  $y$ . There are two obvious options for this,

- Use  $y = 0$ . This is all that can be done when a single BPM is analyzed in isolation, as is done on the front end computers.
- Use the value of  $y$  computed from neighboring BPMs and the knowledge of the lattice, as might be done offline.

## 6 Simulations

The plots in Figure 2 show the results of computations of  $A$  and  $B$  computed using Equations 18 and 19 along with Equations 1 and 2. The values of the

parameters are,  $b = 35$  mm,  $\phi = 110^\circ$  and  $C = 0.11810$ . Both plots show the values of  $A$  and  $B$  as a function of  $x$ , for different values of  $y$  and for different orders of approximation in equations Equations 1 and 2. From this we can see that going from first to third order of approximation makes a large change but that adding further orders makes only a small change.

The plot in Figure 3 shows the results of the following study. For different values of  $x$  and  $y$ ,  $A$  and  $B$  were computed to 11<sup>th</sup> order. These values were used to compute the first order position estimate, Equation 25. The plot shows the difference between the first order  $x$  position estimate and the generated  $x$  position, as a function of generated  $x$  position. This is done for several different values of  $y$ . The horizontal axis covers the full region for which the requirements document specifies an accuracy of less than 1 mm. The first order estimate fails the requirement for large values of  $x$ . Interestingly, the accuracy at large  $x$  is best when  $y$  is also large; this is explained by the relative sign in the  $(x^2 - y^2)$  the  $(x^2 - 3y^2)$  terms in equations 20 and 21.

The procedure was repeated using the ninth or tenth order calculation of  $A$  and  $B$ . In these trials, the estimated position changed by less than 1  $\mu\text{m}$ , relative to the trial at eleventh order. From this we conclude that the computation of  $A$  and  $B$  to eleventh order is more than sufficient to study the quality of the position estimators.

The plots in Figure 4 show the results of computing  $A$  and  $B$  to eleventh order then computing the position to third order, using Equation 36. The upper and lower plots show the same information but with different vertical scales. In order to use this equation, one must supply an estimate for  $y$ . When making this plot, the true value of  $y$  was used. While this does not represent how the instrument can be used in the field, it does provide a baseline against which different algorithms for  $y$  can be benchmarked. This plot shows that if the quality of the  $y$  estimate is excellent, then the worst case bias in the  $x$  position estimate is less than 250  $\mu\text{m}$  over the full range of interest,  $|x| < 15$  mm and  $|y| < 15$  mm.

Figure 5 again shows the results of computing  $A$  and  $B$  to eleventh order then computing the position to third order, using Equation 36. In this case, however, a value of  $y = 0$  was used for computing the estimated position, regardless of the value of  $y$  used to compute  $A$  and  $B$ . Both the upper and lower plots show the same information but on different vertical scales. This calculation simulates a procedure that could be implemented on the front end computers. These plots show that, for  $|y| < 10$  mm, the the bias in  $x$  is less than the requirement of 1 mm for all values of  $|x| < 15$  mm. For  $|y| > 10$  mm, however, the bias is larger than the requirement.

Figure 6 again shows the bias that results from computing  $A$  and  $B$  to eleventh order then computing the position to third order, using Equation 36. For the solid lines, Equation 36 was computed using  $y = y_{\text{gen}} + 1$  mm, where  $y_{\text{gen}}$  is the generated value of  $y$ . For the dashed lines the position was computed using  $y = y_{\text{gen}} - 1$  mm. This procedure models the sort of resolution in  $y$  that might be available offline by using information from neighboring BPMs. The results are excellent: the bias is less than 550  $\mu\text{m}$  over the full range of interest

and less than  $200\text{ }\mu\text{m}$  for  $|y| < 10\text{ mm}$ .

## 7 Summary and Conclusions

Provided that the model of the pickup response and the model of coupling are sufficiently accurate, this note shows that the first order  $x$  position estimate passes the accuracy requirement of  $\pm 1\text{ mm}$  for small values of  $x$  but that it fails the requirement for large values of  $x$ . It also shows that the third order estimate for  $x$ , using  $y = 0$ , meets the requirements over most of the parameter space; it fails only at large  $y$ . Finally, if  $y$  information derived from neighboring BPMs has an accuracy of about  $\pm 1\text{ mm}$ , then the third order  $x$  position estimate, meets the accuracy requirements over the full parameter space.

What remains is to understand if this model of the pickup response and coupling are themselves sufficiently accurate.

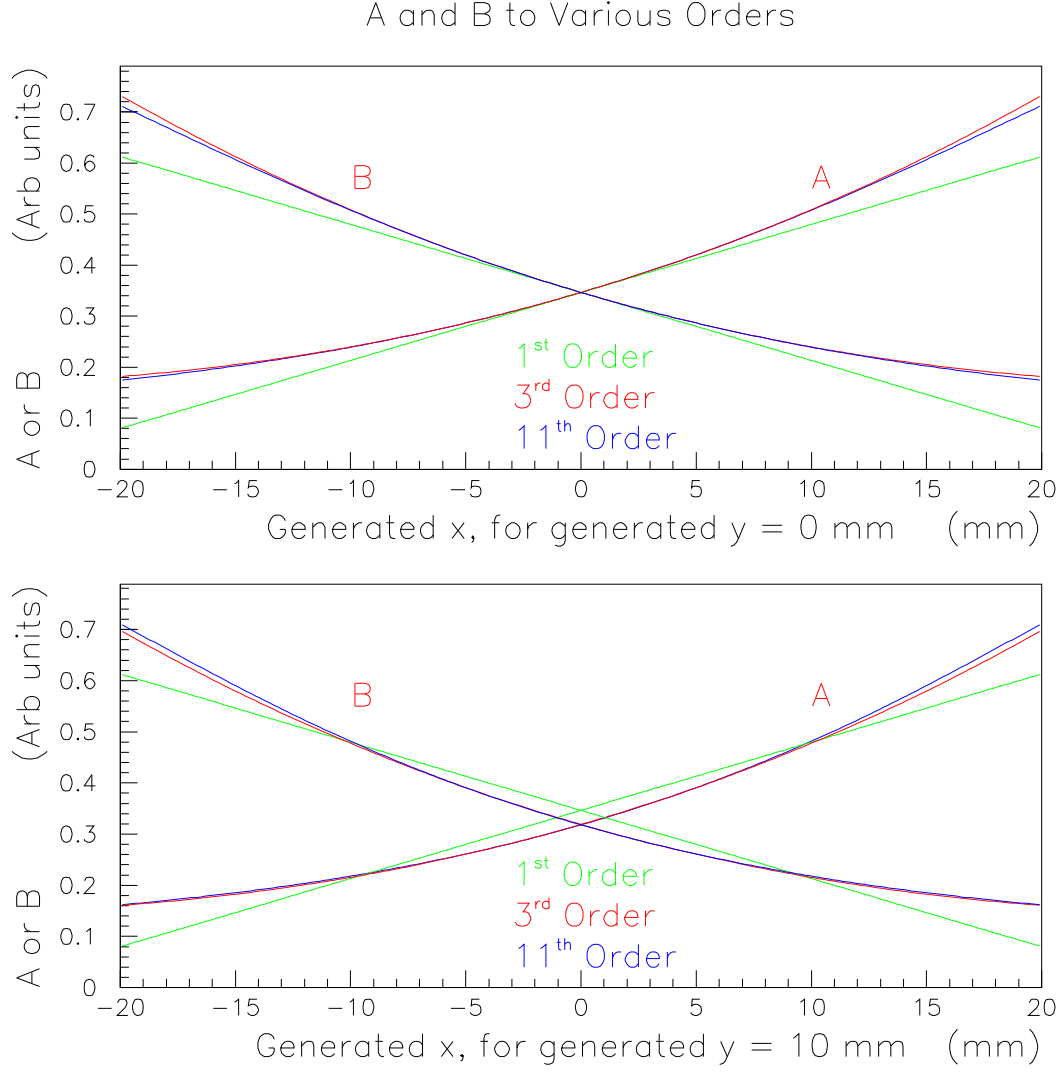


Figure 2: Values for  $A$  and  $B$  computed using the model described in the text. The upper plot shows  $A$  and  $B$  as a function of generated  $x$  for generated  $y = 0$  mm, while the lower plot shows the same quantity for generated  $y = 10$  mm. In each case the three lines show different orders of expansion. By 11<sup>th</sup> order, the expansion has converged at a level corresponding to a position accuracy of better than  $1\text{ }\mu\text{m}$ .



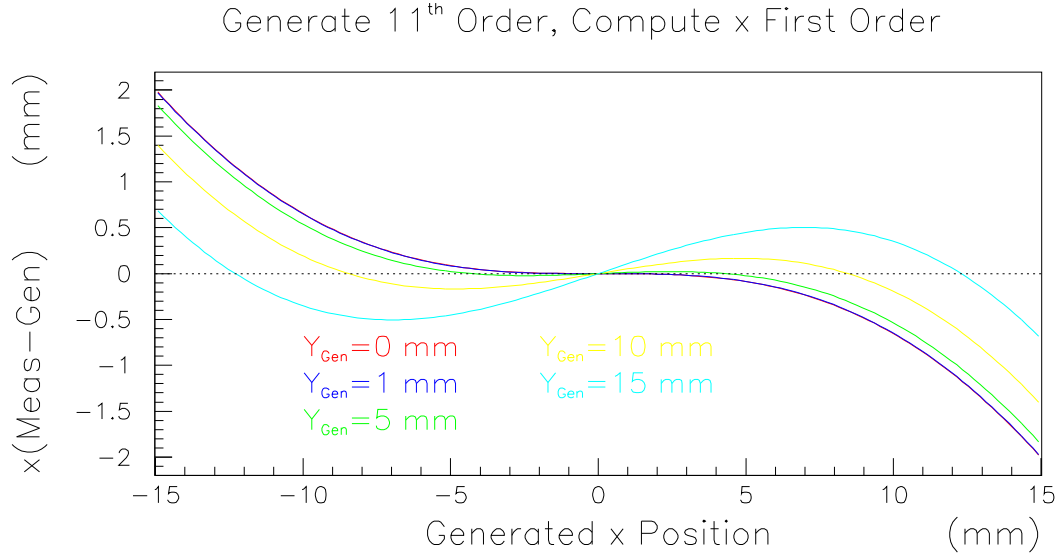


Figure 3: To make this plot  $A$  and  $B$  were computed to 11<sup>th</sup> order using the model described in the text. These values were then used to compute the first order  $x$  position estimate. The plot shows the bias in the first order  $x$  position estimate as a function of the true  $x$  position. The different colors correspond to different values of true  $y$  position. On this scale the red and blue curves are nearly coincident.

Generate 11<sup>th</sup> Order, Compute x Third Order

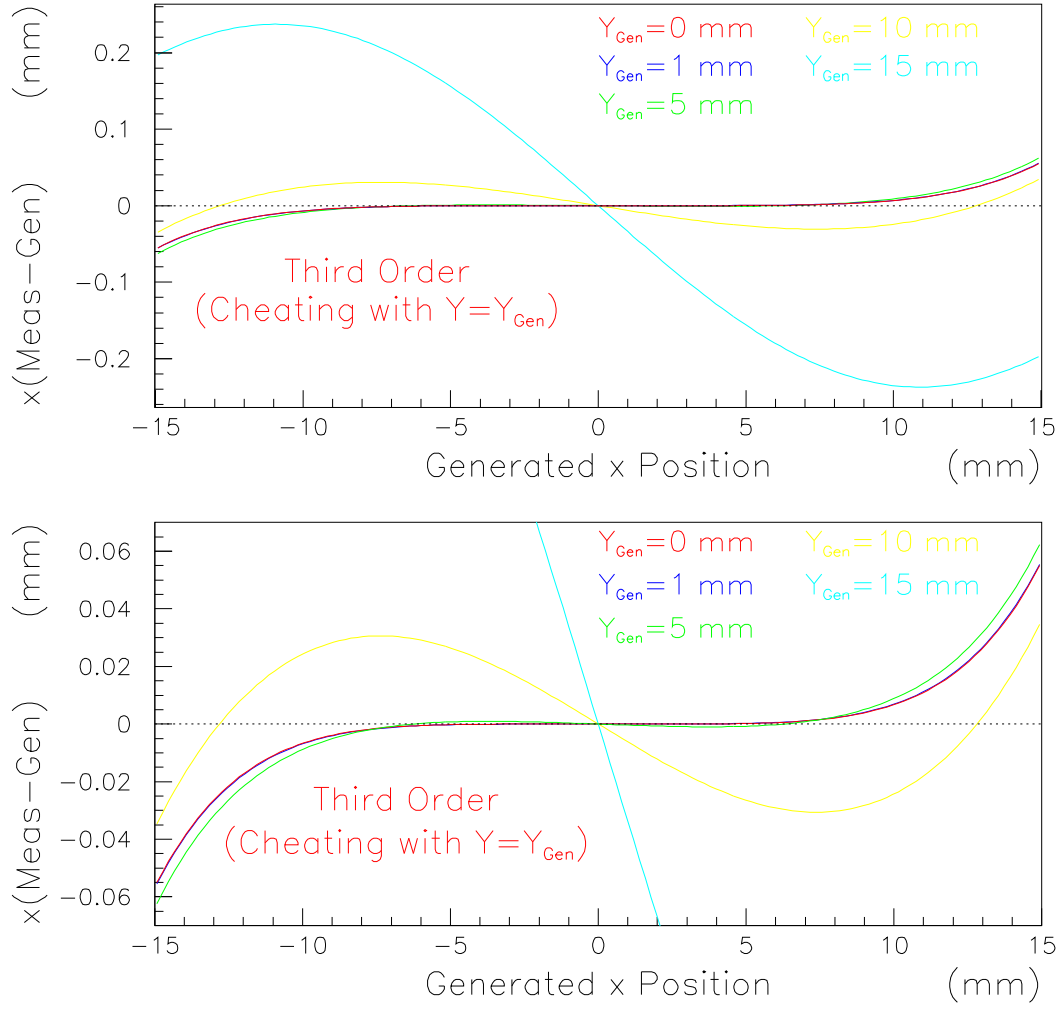


Figure 4: The bias in the third order  $x$  position estimate as a function of the true  $x$  position. The third order  $x$  position estimate was computed with perfect knowledge of the  $y$  position. This scenario will not be achieved in the field but it establishes a useful baseline. The different colors correspond to different values of true  $y$  position. The upper and lower plots show the same information but on different vertical scales. Even on the expanded vertical scale of the bottom plot, the red and blue curves are nearly coincident.

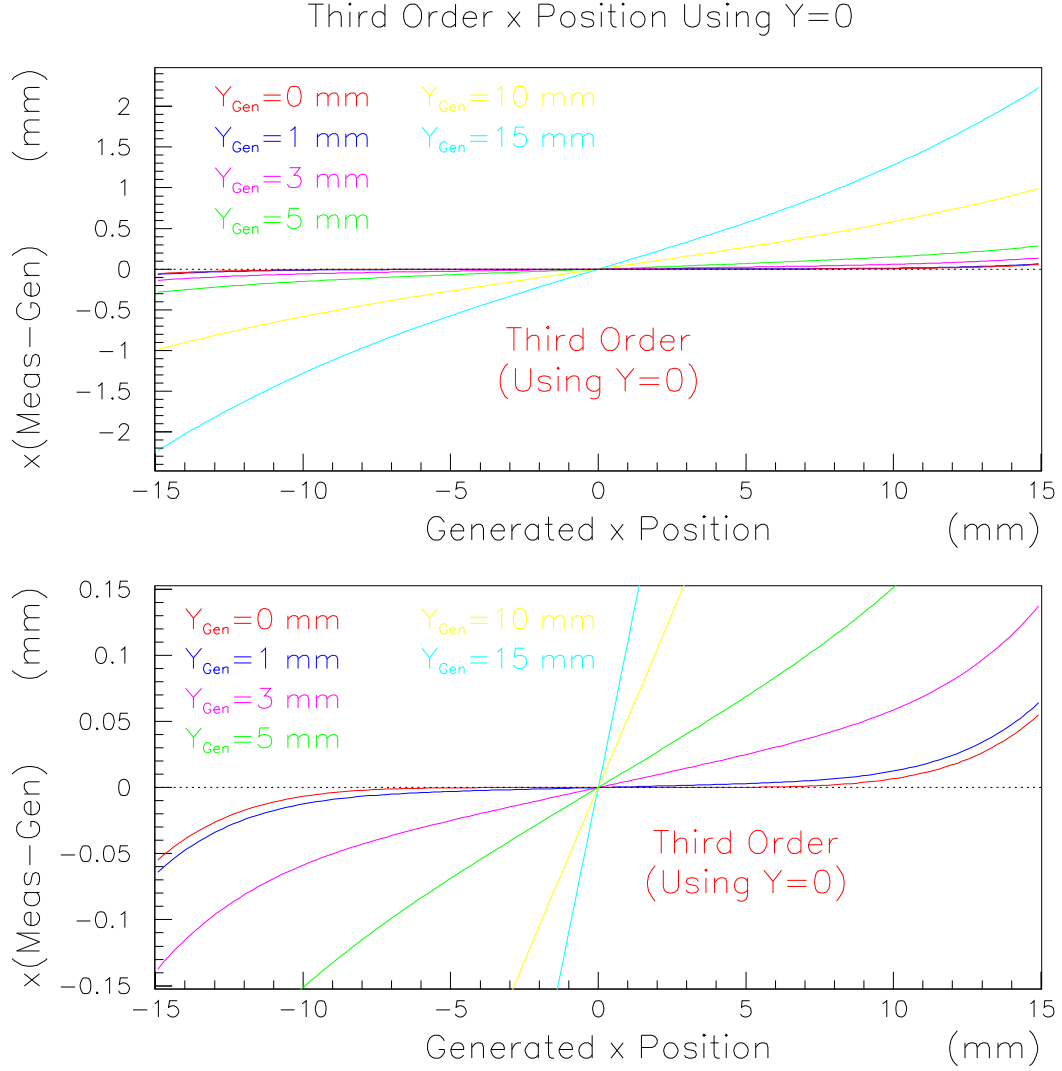


Figure 5: The bias in the third order  $x$  position estimate as a function of the true  $x$  position. The third order  $x$  position estimate was computed using  $y = 0$ , as can be implemented in the front end computers. The different colors correspond to different values of true  $y$  position. The upper and lower plots show the same information but on different vertical scales.

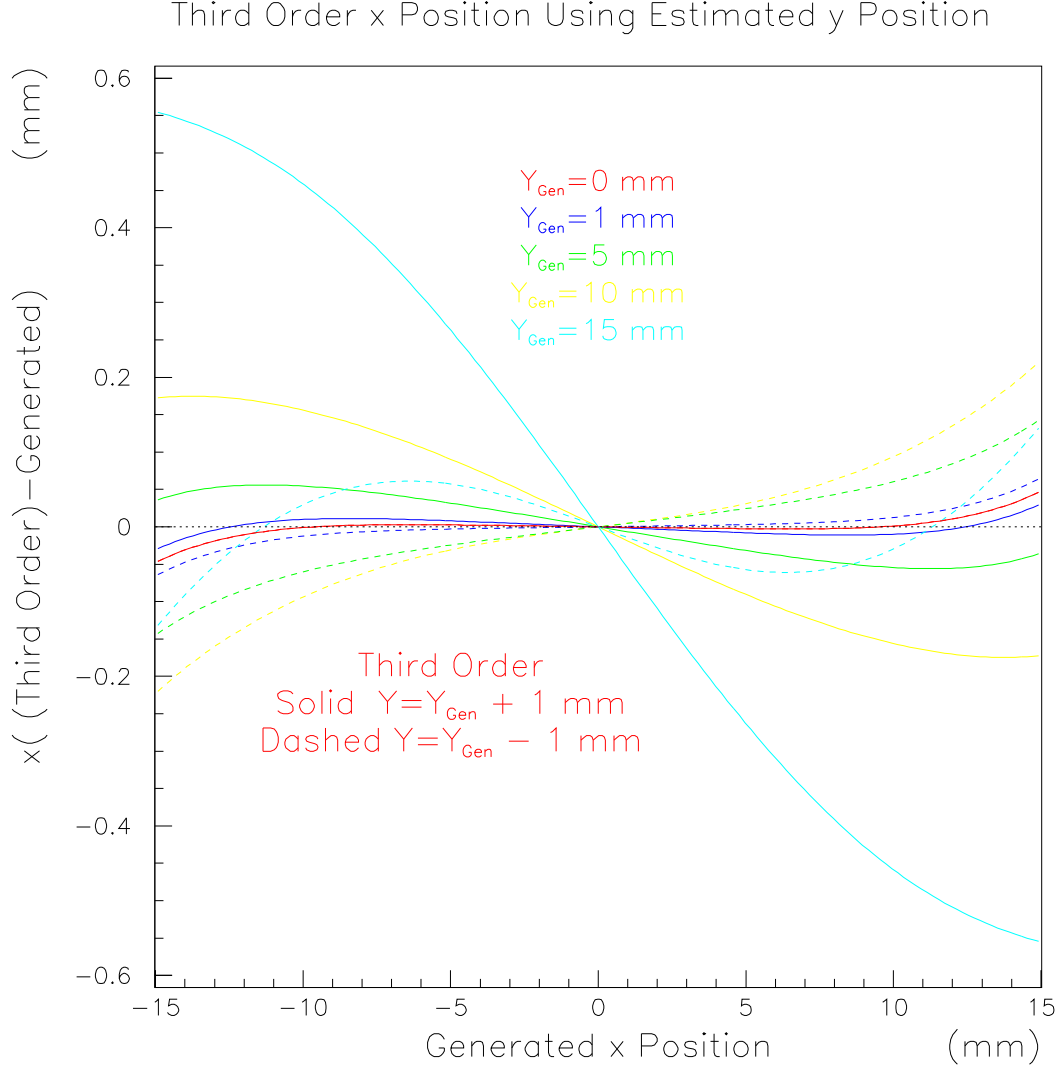


Figure 6: The bias in the third order  $x$  position estimate as a function of the true  $x$  position. The third order  $x$  position estimate was computed using the true value of  $y$  plus a bias of  $+1 \text{ mm}$  (solid) or  $-1 \text{ mm}$  (dashed). This is intended to estimate the bias in  $x$  that might be achieved offline using  $y$  information from neighboring BPMs. The different colors correspond to different values of true  $y$  position.